

Received 14 September 2023, accepted 13 October 2023, date of publication 17 October 2023, date of current version 1 November 2023.

Digital Object Identifier 10.1109/ACCESS.2023.3325292

RESEARCH ARTICLE

Short-Term Solar Irradiance Forecasting Using Deep Learning Techniques: A Comprehensive Case Study

SALWAN TAJJOUR¹, SHYAM SINGH CHANDEL¹, MAJED A. ALOTAIBI²,
HASMAT MALIK^{3,4}, (Senior Member, IEEE), FAUSTO PEDRO GARCÍA MÁRQUEZ⁵,
AND ASYRAF AFTHANORHAN⁶

¹Centre of Excellence in Energy Science and Technology, Shoolini University, Solan 173229, India

²Department of Electrical Engineering, College of Engineering, King Saud University, Riyadh 11421, Saudi Arabia

³Department of Electrical Power Engineering, Faculty of Electrical Engineering, University Teknologi Malaysia (UTM), Johor Bahru 81310, Malaysia

⁴Department of Electrical Engineering, Graphic Era (Deemed to be University), Dehradun 248002, India

⁵Ingenium Research Group, Universidad Castilla-La Mancha, 13071 Ciudad Real, Spain

⁶Faculty of Business and Management, Universiti Sultan Zainal Abidin (UniSZA), Kuala Terengganu, Terengganu 21300, Malaysia

Corresponding authors: Hasmat Malik (hasmat.malik@gmail.com) and Majed A. Alotaibi (majedalotaibi@ksu.edu.sa)

This work was supported by the Researchers Supporting Project at King Saud University, Riyadh, Saudi Arabia, under Project RSP2023R278.

ABSTRACT Reliable estimation of solar irradiance is required for many solar energy applications such as photovoltaics, water heating, cooking, solar microgrids, etc. Deep Learning techniques have shown outstanding behaviour for analysing complex datasets efficiently with high accuracy. Multi-Layer Perceptron (MLP), Long-Short Term Memory (LSTM), and Gated Recurrent Unit (RGU) techniques are found to be the most competitive techniques in the literature for solar irradiance forecasting. Therefore, in this study, a comparative analysis of those models is carried out using eleven years of NASA satellite data for training and testing. The grid search technique is used to optimize the networks architectures to ensure the best performance of the models for forecasting daily global solar irradiance. The results show that all models have similar accuracy with a mean square error close to 0.017 kWh/m²/day. However, the speed of training varies between 17 and 208 seconds for each model where GRU has shown higher speed than LSTM despite of containing more layers due to their computational complexity. The MLP is found to be the most efficient model due to using a low number of parameters 49,281 as compared to 1,025,793 for GRU. The study is of importance for reliable solar irradiance forecasting for any location worldwide.

INDEX TERMS Solar energy, solar irradiance, forecasting, machine learning techniques, artificial neural network.

I. INTRODUCTION

Solar energy is a clean and alternate reliable option to fossil fuels which is being used worldwide. The total energy that reaches the earth from the sun beams is huge ($1 \text{ EJ} = 10^{18} \text{ J}$) [1] whereas only $5 \times 10^4 \text{ EJ}$ is easily harvestable [2]. Several factors like climate, circadian variation, latitude, and geographic change are responsible for the amount of sunlight crossing the atmosphere [3]. The earth's atmosphere receives about 342 W/m^2 of solar energy, of which 30% is scattered

The associate editor coordinating the review of this manuscript and approving it for publication was Ehab Elsayed Elattar⁶.

or reflected in space again, leaving around 70% available for harvesting [4].

The solar irradiance varies due to the earth's rotation around the sun along with other parameters like sun orientation, aerosol, temperature, wind speed, direction and many more variables, thus, solar energy is a non-predictable resource. The solar irradiance datasets are unavailable for most locations worldwide due to the lack of meteorological stations. Therefore, different methods are used to forecast solar irradiance for locations where no measured data are available [5]. Recently Artificial intelligence (AI) techniques are employed extensively to predict solar irradiance and have

been found to give very accurate results [6], [7], in addition, different climate variables are used to predict solar irradiance accurately [8].

As a result of developments in physical modelling (NWP), statistical modelling, and AI, forecasting skill is still improving. The future of forecasting for solar energy has a lot of promise for expanding the kinds and quantities of data utilised in statistical and physical modelling due to the accessibility of big data sets and the inclusion of new data sources. Larger datasets can be utilised to drive newer statistical and machine learning techniques, and new data assimilation techniques will enhance forecast accuracy [9].

Advanced technology will also be needed for managing power systems with significant levels of distributed renewable energy output. Effectively managing power systems with extensive decentralized renewable energy generation necessitates a high level of expertise in forecasting techniques tailored to these energy sources. This includes “behind-the-meter” forecasting and the development of innovative methods for representing forecast uncertainty. Solar energy forecasting, in particular, extensively relies on statistical models and artificial intelligence (AI) [10].

Moreover, the forecasting time horizon is selected based on the requirement where short-term horizons are used for integration of the grid with the PV systems, medium-term horizons are used for system planning and maintenance, and the long-term horizons are used for planning electricity such as distribution and generation [11]. Multi-horizon forecasting is also presented in [12] considering 3/6/24 hours ahead for solar irradiance. Enhancing forecasting accuracy in this context can be achieved by incorporating supplementary data sources like cloud imagery, NWP forecast data, radar information, neighbouring data points, or weather classifications. Additionally, statistical techniques are applied to eliminate systematic biases, translate data into power generation predictions, and precisely measure the degree of uncertainty [13].

Different machine learning (ML) techniques are explored in several studies and compared with other techniques to find the best techniques for further implementation in research and industry [14]. In this study “grid search”, which is an efficient technique is used to optimize the architecture and the training process for ML models, where each hyperparameter is chosen from a list of values that ensures their optimum performance.

The novelty and contributions of this paper are to review the literature and find the most competitive techniques for solar radiation forecasting and then develop an intelligent model for forecasting of daily solar irradiance for a remote location in India, where no weather station is available. Three DL techniques namely Multi-Layer Perceptron (MLP), Long-Short Term Memory (LSTM), and Gated Recurrent Unit (GRU) are found to be the most competitive for global solar irradiance forecasting (SIF) at any location. the grid search technique is used to optimize the network architecture to ensure an unbiased comparison of the models. These models

are trained and tested using daily satellite solar irradiance data.

This study is structured as follows: the literature is reviewed to identify the suitable DL techniques and the evaluation metrics in section II. In section III, a case study is presented in addition to the methodology, followed by the results and discussion of the study in section IV. Moreover, the conclusions and follow-up research areas are presented in section V.

II. LITERATURE REVIEW

Several techniques are used to predict solar irradiance for different solar applications like solar photovoltaic (PV) panels, solar concentrating systems, solar cooking systems, etc. Machine Learning techniques are applied for solar irradiance forecasting (SIF) due to their unbeatable performance in solving complex problems. The most important predictors to train artificial neural networks (ANNs) for SIF are investigated in [15], which boosts the training time and accuracy. Yadav et al. [16] 26 locations are studied considering different climatic regions. The authors used WEKA for feature selection [17]. They also used the rapid miner technique for feature selection in other research for 76 locations in India [18], whereas maximum/minimum temperature, altitude, and sunshine hours are found to have a significant impact on the training process.

Voyant et al. [19] reviewed different ML techniques in addition to statistical methods and found that SVM, Decision Tree (DT), and Random Forest (RF), are the most convenient techniques for this task as these are easy to build and perform similarly as complex techniques as ANN or Autoregressive integrated moving average (ARIMA). A comparative study between different hybrid models is presented in [20], in order to explore their applications and to identify the best models for SIF. The study is divided based on the ensemble learning approaches and found that Decomposition-Clustering based ensemble learning approach (DCELA) is the best combination technique for SIF. An overview of SIF methods for different time horizons is presented in [21], whereas solar irradiance resources, sensor datasets, radiometers, and forecast error metrics are reviewed. In [22] a comparison between conventional ML techniques and DL techniques for GHI and diffuse solar irradiance is carried out for four locations in Nigeria with hourly time horizon forecasts. DL techniques are found to take more training time but give more accurate predictions.

Rajagukguk et al. [23] compared some deep learning techniques namely Recurrent Neural Network (RNN), LSTM, GRU and a hybrid technique of Convolutional Neural Network CNN and LSTM based on the accuracy, input parameters, time horizon, training time, and type of season and weather. CNN-LSTM model is found to outperform the other models; however, it needs a longer convergence time. Furthermore, an analysis of different physical, statistical, ML models, and the hybrid approach, is presented in [24]. The study found that ML techniques are more complicated than statistical ones, however, ML gives higher accuracy.

In addition, numerical weather prediction methods are too sophisticated to be understood. Furthermore, ensemble models can overcome uncertainty in the data to give more precise results.

Different types of ML techniques are utilized for predicting GHI on horizontal surfaces such as, SVM, RF, linear regression (LR), DT, polynomial regression (PR), and K-Nearest neighbour (K-NN) [25], [26], [27]. More deep neural networks like CNN, RNN, and Radial basis function neural network (RBFNN) are adopted for this problem [28], [29], [30], [31], [32].

A Bayesian model averaging (BMA) for monthly SIF in Turkey is presented in [33]. BMA is found to be more accurate than Weight Agnostic Neural Networks (WANN), Weighted extreme learning machine (WELM) and wavelet transform based on RBFNN. Moreover, ANN is found to be superior to DL, SVM, KNN to find daily solar irradiance forecasts in Turkey [34]. Moreover, six different techniques (multilayer perceptron (MLP), gradient boosting tree (GBT), two types of adaptive neuro-fuzzy inference systems (ANFIS), Multivariate adaptive regression spline (MARS), classification and regression tree (CART)) are used for daily SIF whereas GBT is performed the best [35]. LSTM is compared to ARIMA, SVR, BPNN and RNN models in [36] and found that LSTM is the best model among them especially in the cloudy and mixed days. Furthermore, RNN, LSTM, FFNN, and GRU are compared to traditional techniques like RFR and SVR in [37]. LSTM and GRU are found to be the best among the other techniques.

Decomposition techniques are also used to analyse solar irradiance data as it is non-stationary and non-linear data. Therefore, techniques like Wavelet Decomposition, Ensemble Empirical Mode Decomposition and Mode Decomposition are used to split the source data into many components [38].

Researchers also used satellite data for solar irradiance analysis and prediction for places at which measured datasets are not available [39]. Both measured and satellite data are used to predict the GHI in Iran [40]. Angstrom exponent, aerosol optical depth, cloud optical depth, cloud fraction, and precipitable water vapour amount are taken from Moderate Resolution Imaging Spectroradiometer (MODIS) instruments in addition to the daily pyrhelimeter measurements GHI. They found that using cloud fraction added valuable parameters to slightly increase the accuracy of the used models (ANN and LR). Images are also used for cloud tracking because its significant impact on climate studies. Therefore, satellite images are used for tracking the clouds in particular regions [41]. In addition, ground-based sky images are used for intra-hours forecasts where satellite images are not suitable [42].

Hybrid techniques, which utilize different techniques like ML, DL, metaheuristics, etc., to achieve more reliable and accurate models [43]. For instance, particle swarm optimization (PSO) is combined with extreme learning machine is proposed in [44]. In [45] self-organizing maps (SOM) is used

for clustering the dataset into similar regions, SVR is used for modelling each cluster and PSO techniques is used to optimize the SVR parameters. Another hybrid spatiotemporal method is proposed in [46] and [46] for day-ahead SIF. This technique uses discrete Fourier transform to extract frequency features from the data, principal component analysis for feature selection and Elman-based neural network for forecasting. A fuzzy regression functions combined with SVM are compared to an ANFIS and a coplot supported-genetic programming approach [47]. In addition, a Hidden Markov Model combined with Generalized Fuzzy technique is compared to ANFIS and ANN for SIF in [48] and found to be more efficient. Evolutionary techniques are used frequently in the literature either by optimizing other techniques' parameters or as hybrid techniques. In [49] Extreme Gradient Boosting (XGB) combined with Genetic Algorithm (GA) and used to forecast solar irradiation using measured data from three different locations in USA.

However, a critical challenge in forecasting lies in instances where the trained model exhibits enduring error patterns, which can be seen as a bias reduction function. This error data can be leveraged for constructing a bias correction model, which can take the form of a straightforward mathematical function or even a complex machine learning algorithm. This developed model is subsequently employed to mitigate the identified bias from the forecasts, resulting in an augmented level of forecasting precision.

Table 1 presents the highlights and the results of the latest publications that used ML techniques for SIF. As shown in the table, DL techniques such as MLP, LSTM, and GRU networks are frequently used in literature and achieved a very good performance; therefore, these techniques will be chosen for more investigations and validation.

A. IDENTIFIED RESEARCH GAPS

Based on the available state-of-the-art, the following research gaps have been identified:

- a) Optimal architecture for models is as important as optimizing the weights, and most of the previous studies did not consider that before comparing between networks.
- b) Hybrid models are sophisticated and difficult to implement and most of these require more time than the stand-alone models as more computations are required. Therefore, optimizing the stand-alone model's architecture could increase the accuracy to match the hybrid model's accuracy but with less complexity.
- c) The models are sensitive to sudden fluctuations in environmental conditions due to the lack of data pre-processing in addition to the volatility of the solar data which already exists.

III. CASE STUDY SOLAR IRRADIANCE FORECASTING FOR A LOCATION IN INDIA

In this section, a location in Bajhol, Solan, Himachal Pradesh, India, is presented as a case study because the authors are conducting research related to solar applications in this part

TABLE 1. Main highlights of the recent publications on solar irradiance forecasting.

Ref	Highlights	Results
[22]	<ul style="list-style-type: none"> Daily forecasting of GSI is presented Actual Data for four locations in Turkey are used Parameters: minimum/maximum temperature, Cloud, extraterrestrial solar irradiance, Day length, Solar irradiance. Techniques: SVM, ANN, k-NN, DL 	<ul style="list-style-type: none"> Metrics used: R, RMSE, NMBE, MAE, MBE, MABE, t-stat, MAPE KNN behaves the worst ANN is found the best fitting algorithm
[34]	<ul style="list-style-type: none"> Daily forecasting of GSI is presented Locations in Turkey, and USA are studied Parameters: wind speed, maximum/minimum temperature, relative humidity Techniques: GBT, ANFIS-SC, ANFIS-FCM, MARS, MLPNN, CART 	<ul style="list-style-type: none"> Metrics used: RMSE, R, MAE, Nash Sutcliffe efficiency coefficient (NS) GBT model performed better than other models
[35]	<ul style="list-style-type: none"> Daily forecasting of GSI and PV power generation discussed Seven stations in China are studied Parameters: full climatic data Techniques: PSO-ELM, ELM, M5 model, SVM, generalized regression neural networks, tree, and autoencoder 	<ul style="list-style-type: none"> Metrics used: MAE, RRMSE, NS PSO-ELM provided more accurate forecasts
[44]	<ul style="list-style-type: none"> Daily forecasting of GSI is presented Actual Data for four locations in Turkey are used Parameters: minimum/maximum temperature, Cloud, extraterrestrial solar irradiance, Day length, Solar irradiance. Techniques: SVM, ANN, k-NN, DL 	<ul style="list-style-type: none"> Metrics used: R, RMSE, NMBE, MAE, MBE, MABE, t-stat, MAPE KNN behaves the worst ANN is found the best fitting algorithm
[46]	<ul style="list-style-type: none"> Day-ahead SIF presented Hybrid spatiotemporal method is proposed. Frequency features are extracted using DFT and then feature selection using PCA. Techniques: Elman-based neural network for forecasting. 	<ul style="list-style-type: none"> Proposed model is compared to the persistence method, ARIMA, PCA-BP-NN, DFT-PCA-BP The most accurate method is found to be DFT-PCA-Elman
[36]	<ul style="list-style-type: none"> Daily and hourly SIF is proposed Techniques: LSTM is compared to ARIMA, SVR, BPNN and RNN Dataset are collected from Atlanta, New York, and Hawaii 	<ul style="list-style-type: none"> K-NN is used to divide data into cloudy, sunny, and mixed days LSTM is the best model among the others especially in cloudy and mixed days
[37]	<ul style="list-style-type: none"> Hourly and daily SIF is proposed for one year ahead Techniques: a comparison of FFNN, RNN, LSTM, and GRU with traditional techniques like RFR and SVR 	<ul style="list-style-type: none"> DL is found to always outperform the traditional techniques LSTM and GRU are found to be the best among the other DL techniques GRU achieved slightly better performance than

TABLE 1. (Continued.) Main highlights of the recent publications on solar irradiance forecasting.

[38]	<ul style="list-style-type: none"> WD, EEMD and EMD are used to build different components and residuals from the source data Actual 1-hour sampled data in France is used Techniques: AR and NN are used for forecasting 	<ul style="list-style-type: none"> LSTM in term of results and speed Found that using wavelet decomposition boosted the performance significantly
[45]	<ul style="list-style-type: none"> Hourly GSI forecasting done Hybrid model of self-organizing maps, SVR and PSO techniques is proposed Colorado, USA and Singapore. 	<ul style="list-style-type: none"> ARIMA, SES, LES, and RW are compared to the hybrid model Hybrid model is found to outperform than other models

TABLE 2. Evaluation metrics used.

Metric	Equation
MAE	$\frac{1}{S} \sum_{j=1}^S Pred(j) - Act(j) $
MSE	$\frac{1}{S} \sum_{j=1}^S (Pred(j) - Act(j))^2$
RMSE	$\sqrt{\frac{1}{S} \sum_{j=1}^S (Pred(j) - Act(j))^2}$
nRMSE	$\frac{\sqrt{\frac{1}{S} \sum_{j=1}^S (Pred(j) - Act(j))^2}}{\overline{Act}}$
MBE	$\frac{1}{S} \sum_{j=1}^S (Pred(j) - Act(j))$

of India, where no measured data are available at present, and the forecast of solar irradiance is required for research and different solar applications.

A. EVALUATION METRICS

The selected metrics (MAE, MBE, MSE, RMSE, nRMSE) are mostly used to evaluate ML models especially in regression problems where, mean absolute error (MAE) measures the prediction error average using the absolute value. Mean biased error (MBE) measure the average bias in the prediction to underestimate/overestimate the measurement. Moreover, root mean square error (RMSE) measures how much predictions differ from measurements. This study follows the same evaluation metrics which are shown in table 2 where S is the number of samples, $Pred(j)$ is the prediction j, $Act(j)$ the real data point j, and $\overline{Act} = \frac{1}{S} \sum_{j=1}^S Act(j)$.

B. MATERIAL AND METHODS

The methodology followed is explained in the flow chart shown in figure 1. Three different Deep Learning networks are chosen from the literature as the most reliable and

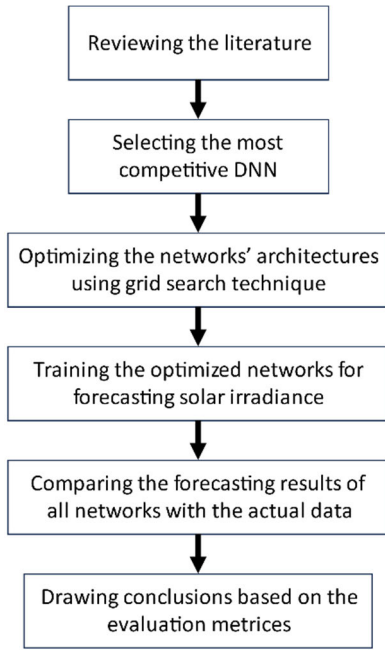


FIGURE 1. Flow chart of the study.

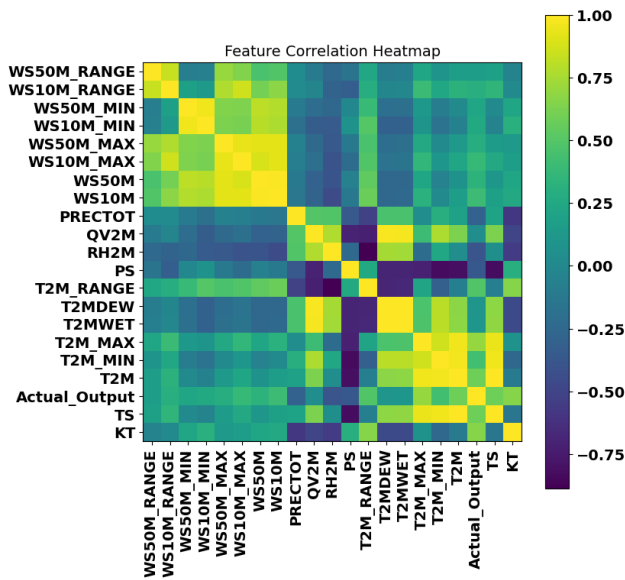


FIGURE 2. The feature correlation heat map of the inputs.

accurate methods for time series problems and especially for solar irradiance prediction. These algorithms are investigated to find the competitive model to forecast the daily GHI. The networks architectures are optimized using the grid search technique. Google Collaboration platform is used for programming purposes of all models using python language. Actual datasets taken from the site are most likely to achieve higher accuracy with a minimum of one year of training samples. However, in this location there are no meteorological data are available so that the satellite data for the last eleven years are utilized. Then the performance of the state-of-the-art ML techniques is investigated and compared.

TABLE 3. Statistical description of the input parameters.

Symbol	PARAMETER	Min	Max	Mean	Std	Unit
WS10M	Wind Speed (WS) at 10m	0.8	7.1	2.6	0.77	m.s ⁻¹
WS50M	WS at 50m	1.1	9.2	3.5	1.1	m.s ⁻¹
WS50M_MIN	Minimum WS at 50 Meters	0.0	6.7	1.6	1.1	m.s ⁻¹
WS50M_MAX	Maximum WS at 50 Meters,	2.1	15	5.2	1.6	m.s ⁻¹
WS10M_MIN	Minimum WS at 10 Meters,	0.0	3.81	1.1	1.1	m.s ⁻¹
WS10M_MAX	Maximum WS at 10 Meters,	1.6	11.8	4.4	1.4	m.s ⁻¹
WS10M_RANGE	WS Range at 10 Meters	0.6	10.8	3.3	1.1	m.s ⁻¹
TS	Earth Skin Temperature	1.3	35.1	19.1	7.7	°C
T2MDEW	Dew/Frost Point at 2 Meters	-9.2	23.7	9	8.5	°C
T2MWET	Wet Bulb Temperature at 2 Meters	-8.5	23.6	9.1	8.4	°C
T2M_RANGE	Temperature Range at 2 Meters	2	21	11	3.4	°C
T2M	Current Temperature at 2 Meters	3.8	33	19.8	6.6	°C
T2M_MAX	Maximum Temperature at 2 Meters	7.3	41.6	26	6.5	°C
T2M_MIN	Minimum Temperature at 2 Meters	-1.3	28	15	6.3	°C
PRECTOT	Precipitation	0	120.7	3.5	8.2	mm.day ⁻¹
QV2M	Specific Humidity at 2 Meters	2.1	21	9.4	5.3	g/kg
KT	Insolation Clearness Index	0.0	0.8	0.56	0.15	dimensionless
PS	Surface Pressure	87.9	90.2	89.2	0.5	kPa

C. DATASET USED

Eleven years of satellite data are used for the location Bajhol, Solan, Himachal Pradesh (Latitude 30.8644N, Longitude 77.1184E) for the period from 2010/05/01 to 2021/05/01. Table 3 represents the parameters used in the data set with

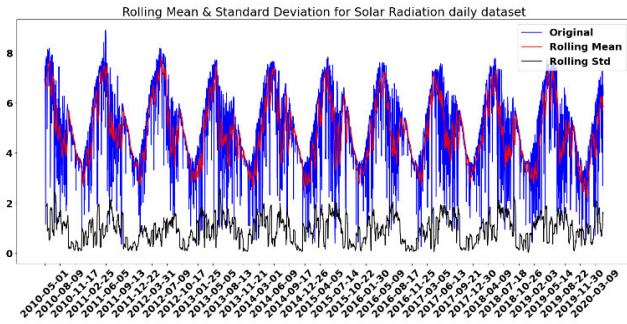


FIGURE 3. Rolling (mean and standard deviation) of the solar irradiance daily measurements combined with the original measurements.

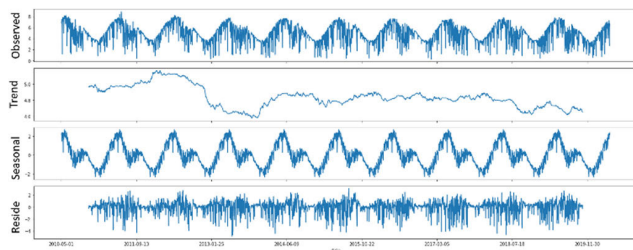


FIGURE 4. Decomposition of the original solar irradiance data into trend, seasonal and residual.

the statistical description of each one including the minimum, maximum, mean and standard deviation.

Pearson correlation coefficient is applied in order to find how variables are correlated to each other's. Figure 2 displays the heatmap of the correlations for all parameters. Clearness index and temperature are most correlated inputs that have significant impact to find the value of solar irradiance, whereas less impact is found for the pressure and humidity.

The original dataset is plotted in figure 3 in addition to the rolling mean and std to give good inspiration for understanding the problem. The daily solar irradiance fluctuates during the time of the year which makes it difficult to predict. By visually checking the dataset it can be observed that the mean and the variance are not constant which means the data is not stationary, and the data obviously has a seasonality trend where the same pattern repeats itself every year with a little difference from the previous year. This has been verified computationally by decomposing the data into trends, seasonal trends and residuals as shown in figure 4.

D. GRID SEARCH TECHNIQUE

The procedure of training for all the proposed networks will follow the same strategy to ensure getting the maximum outcome from every network and for that the size of the window is fixed to consider only the very last 5 samples in the data. As choosing the optimal architecture is a tough task for most of the problems, many techniques are used to find the optimal architecture automatically due to the problem itself. One of the techniques is called grid search which is a useful technique that can search automatically through a limited range of possible choices (grid) and then it converges

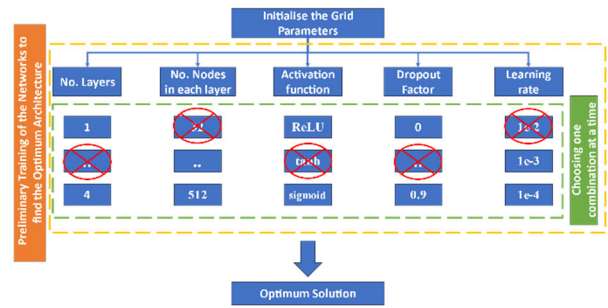


FIGURE 5. Grid search strategy.

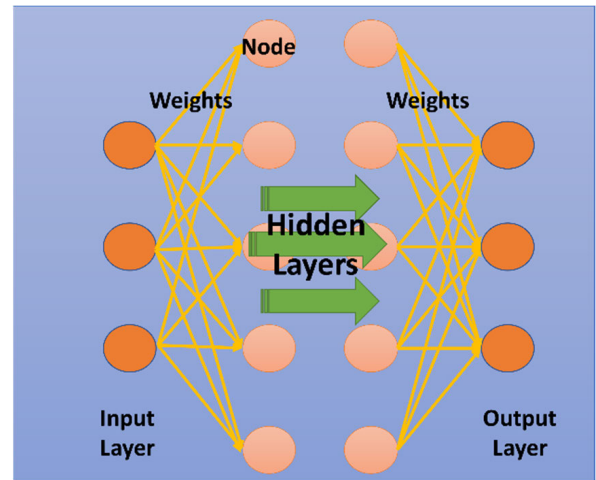


FIGURE 6. MLP architecture.

on the best architecture, among the other options, at which the network gives the maximum accuracy. This grid search technique is explained in figure 5 where the algorithm tries to change the parameters values within the specified range to converge on the best solution that gives the least error. In this study, grid search is used to optimize the layers' number (set from 1 to 4), the nodes' number in each layer (set from 32 to 512 for each layer), the learning rate chosen from the list (1e-2, 1e-3, 1e-4), the dropout factor should be less than 0.9 and the activation functions for each layer which could be 'Relu', 'tanh' or 'sigmoid' except the last layer which has linear activation function. For evaluation purposes the last year's data are held for testing and evaluating of the model.

E. MULTI-LAYER PERCEPTRON

The main concept behind ANNs is to mimic the behaviour of the brain whenever it wants to understand or recognize anything and the way it makes reasonable decisions. MLP architecture, shown in figure 6, contains multiple layers, these layers have nodes, the nodes relate to each others using weighted paths represent the way of the thinking where those weights will be trained, and their values will be optimized to deal with the dedicated problems [50], [51].

The feed forward calculations are shown in (1) where h_t^j is the output of the j-th node at time t, θ is the activation

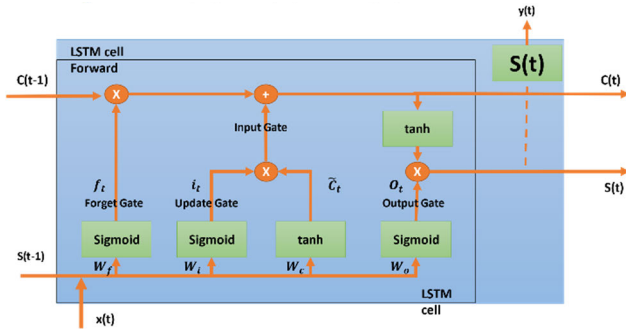


FIGURE 7. LSTM architecture.

function, W_t^j is the weights, X_t^j is the inputs, B_t^j is the biases.

$$h_t^j = \theta(W_t^j * X_t^j + B_t^j) \quad (1)$$

F. LONG SHORT-TERM MEMORY

LSTM is a special network built out of RNN which is similar to MLP, however, it has memory that gives the ability to such networks to remember previous data. The aforementioned feature of LSTM makes it suitable for time series problems where the current observation is strongly dependent on the previous ones. LSTM architecture, as shown in figure 7, contains cells which are able to remember previous observations over arbitrary time intervals. Input, output and forget gates control the data flow in and out the cell [52].

The feed forward calculations are shown in (2)-(7) for the j -th LSTM unit, S_t^j is the output, O_t^j is the output gate, C_t^j is the memory, f_t the forget gate, i_t^j the input gate, σ is the sigmoid function, \tilde{C}_t^j is the updated memory, V_o , V_i and V_c the diagonal matrices

$$S_t^j = O_t^j \tanh(C_t^j) \quad (2)$$

$$O_t^j = \sigma(W_o x_t + U_o S_{t-1} + V_o C_t^j) \quad (3)$$

$$C_t^j = f_t^j C_{t-1}^j + i_t^j \tilde{C}_t^j \quad (4)$$

$$\tilde{C}_t^j = \tanh(W_c x_t + U_c S_{t-1}) \quad (5)$$

$$f_t^j = \sigma(W_f x_t + U_f S_{t-1} + V_f C_{t-1}^j) \quad (6)$$

$$i_t^j = \sigma(W_i x_t + U_i S_{t-1} + V_i C_{t-1}^j) \quad (7)$$

G. GATED RECURRENT UNITS

GRU is similar to LSTM but with a smaller number of hyperparameters as it contains only reset and update gates as shown in figure 8. Reset gate decides if the information from previous state have to be included or not, whereas Update gate determines the information to be passed to the current state. If the Reset gate value is "0" then the current hidden state will ignore the information from the previous state [53]. The feed forward calculations are shown in (8)-(11), where z_t^j is the update gate, r_t^j is the reset gate, \odot element wise

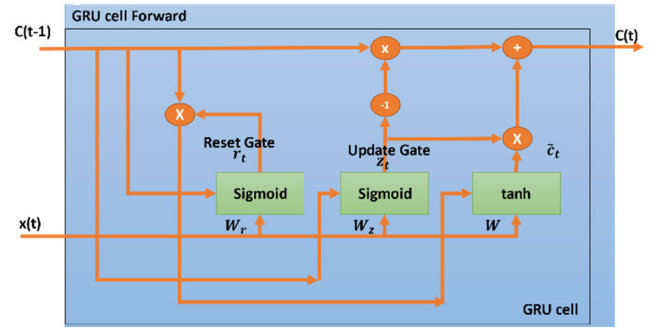


FIGURE 8. Gated Recurrent Unit architecture.

multiplication, and σ sigmoid function.

$$C_t^j = (1 - z_t^j) C_{t-1}^j + z_t^j \tilde{C}_t^j \quad (8)$$

$$z_t^j = \sigma(W_z x_t + U_z C_{t-1}^j) \quad (9)$$

$$\tilde{C}_t^j = \tanh(W_c x_t + r_t^j \odot (U_c C_{t-1}^j)) \quad (10)$$

$$r_t^j = \sigma(W_r x_t + U_r C_{t-1}^j) \quad (11)$$

IV. RESULTS AND DISCUSSION

MLP, LSTM and GRU results comparison is presented in this section where Google Collabs platform is used for developing all the models using Python. The forecasting results based on the 11 years of daily solar irradiance data that is divided into 10 years for training and 1 year for testing. Before training the data is normalised between 0 and 1 using minmax scaler. The networks are trained after optimizing their architectures using the grid search strategy and the results are discussed in this section.

MLP best architecture is found to contain one layer only with 352 number of neurons and the model achieved 0.0171 MSE and 0.095 MAE. On the other hand, LSTM network best architecture is found to have two layers with [64, 256] units which makes the number of hyperparameters of this network is high and achieved 0.0173 MSE and 0.092 MAE. Moreover, the optimum architecture of the GRU network is found to be the deepest with three layers including [192, 256, 320] units respectively which makes the number of hyperparameters of this network high. The model achieved 0.0172 MSE and 0.091 MAE. In terms of complexity, MLP is the simplest network amongst all of three networks as the total number of parameters is 49281 which is 7 times less than LSTM and 20 times less than GRU. The number of parameters of LSTM is about 7 times more than that of MLP, and for GRU its about 21 times more than MLP. This is because of the number of layers and units used in each of them.

The behaviours of MLP, LSTM and GRU are displayed in figures 9, 10, 11 respectively, where the actual dataset is shown in orange and the predictions are shown in blue colours. This is done for the last year of the dataset, and it could be estimated visually that all networks behave the same and the average prediction is less than the actual data. However, the

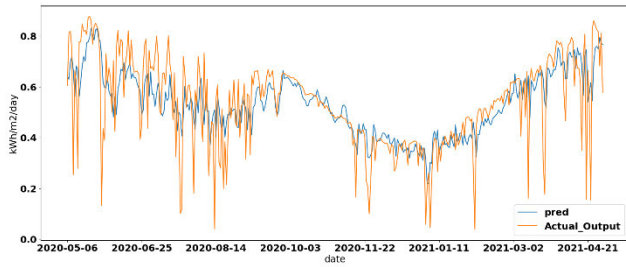


FIGURE 9. Measured output (orange) and the predicted (blue) values by MLP.

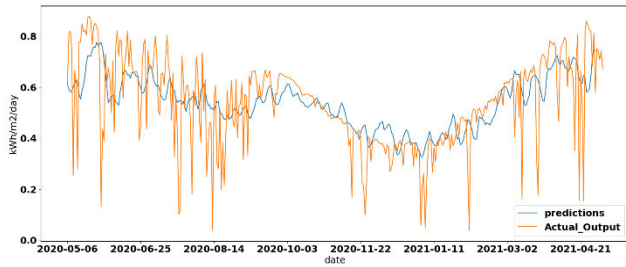


FIGURE 10. Measured output (orange) and the predicted (blue) values by LSTM.

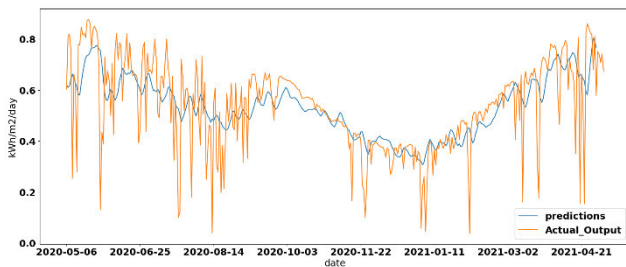


FIGURE 11. Measured output (orange) and the predicted (blue) values using GRU.

TABLE 4. Evaluation results of the three networks.

Metrices and indicators	MLP	LSTM	GRU
No. of neurons in each layer	[352]	[64, 256]	[192, 256, 320]
No. of parameters	49,281	351,489	1,025,793
No. of training epochs	81	514	44
Training time	17 S	208 S	21 S
MSE (kWh/m2/day)	0.0171	0.0173	0.0172
RMSE (kWh/m2/day)	0.13	0.132	0.131
nRMSE (kWh/m2/day)	0.156	0.157	0.156
MBE (kWh/m2/day)	-0.012	-0.0058	-0.0056
MAE (kWh/m2/day)	0.095	0.092	0.091

models can follow the pattern of the original data with minor fluctuations.

R value which shows the relation between predictions and actual values are found to be 0.61, 0.65, and 0.7 for the models LSTM, GRU, and MLP respectively. This shows that MLP is the most accurate model. Figures 12,13,14 show

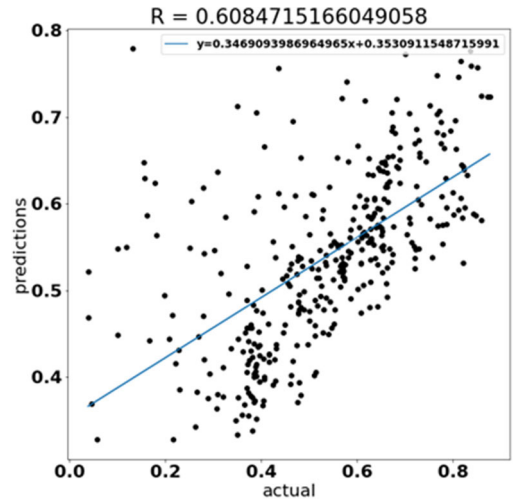


FIGURE 12. Scatter plot and the R-value of LSTM predictions and actual values with linear regression line.

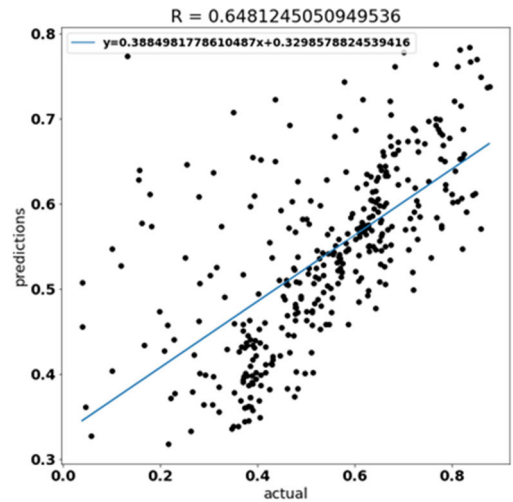


FIGURE 13. Scatter plot and the R-value of GRU predictions and actual values with linear regression line.

the predictions and real values of the daily solar irradiance considering the test set only which also show how accurate are the models.

As shown in table 4, all the three networks achieved around 0.017 MSE, 0.13 RMSE, 0.16 nRMSE and 0.09 MAE; however, MLP achieved slightly more MBE (0.01) than (0.006) for LSTM and GRU. The value of MBE is always negative for all these methods which shows that the solar irradiance is usually underestimated. MLP is the fastest network to converge within only 17 seconds and 81 epochs. However, it is important to mention that GRU shows interesting behaviour as it has the largest number of parameters yet there are only 5 seconds difference to MLP convergence time and still faster than LSTM due to a smaller number of gates which means less matrix multiplications. By considering all parameters, MLP is the best network because it gives the same accuracy

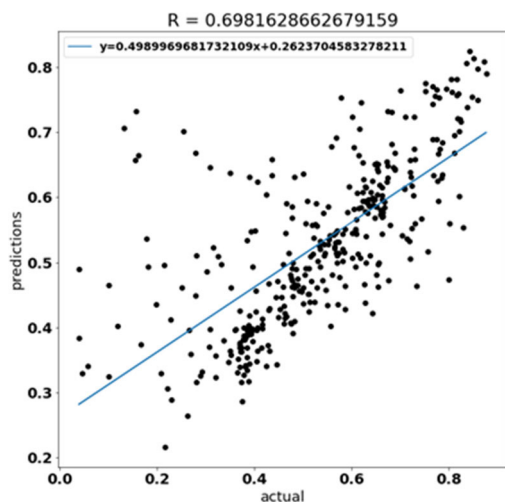


FIGURE 14. Scatter plot and the R-value of MLP predictions and actual values with linear regression line.

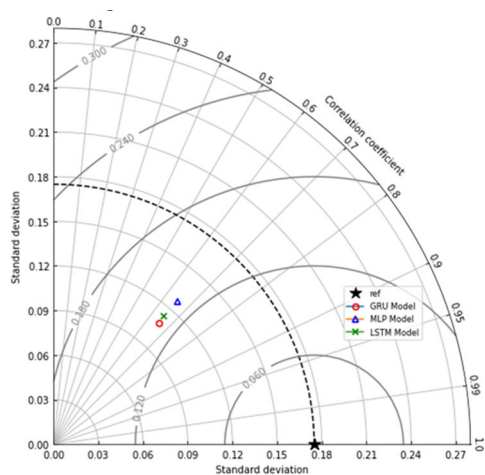


FIGURE 15. Taylor diagram of all models' predictions compared to the reference data.

within less time. Furthermore, MLP can be implemented in an embedded systems with low configuration as it does not require high storage and the computational complexity is less.

Figure 15 represents Taylor diagram which displays the difference between the models based on three metrics including CC, STD, and centered RMSE. As shown in the figure, all models have similar behaviour in term of CC and RMSEc however, MLP model has closer STD to the reference one than other models.

The low number of layers found in all networks can be due to the dataset size which might not be enough to train deeper networks. On the other hand, simple tasks or tasks with short-range dependencies may not require the complexity of deep recurrent architectures. This may make the MLP shallow network, with feedforward connections, suffice for tasks that do not involve capturing complex sequential patterns.

Data preprocessing and feature engineering also play a crucial role in the performance of deep neural networks. A shallow MLP might be more forgiving when it comes to

TABLE 5. A comparison of present study results with other studies from the literature.

Ref	Parameters	Time horizon	Model	RMSE (W/m ²)
[54]	<ul style="list-style-type: none"> • Temperature • Dew Point • Humidity 	Day	LSTM	76.245
[55]	<ul style="list-style-type: none"> • GHI • Solar zenith angle 	Hour	LSTM GRU	<ul style="list-style-type: none"> • 66.57 • 67.29
[56]	<ul style="list-style-type: none"> • Temperature • Humidity • Cloud cover 	Day	LSTM	62.54
[57]	<ul style="list-style-type: none"> • Temperature • Humidity • Precipitation 	Day	LSTM	60.31
[58]	<ul style="list-style-type: none"> • Solar irradiance 	5-min		<ul style="list-style-type: none"> • 18.85 • 20.75
		10-min	LSTM GRU	<ul style="list-style-type: none"> • 14.2 • 15.2
		20-min		<ul style="list-style-type: none"> • 33.86 • 29.58
		30-min		<ul style="list-style-type: none"> • 58 • 55.29
This Work	<ul style="list-style-type: none"> • Wind speed and direction • Temperature • clear-sky index • Humidity 	Day	<ul style="list-style-type: none"> • LSTM • GRU • MLP 	<ul style="list-style-type: none"> • 12 • 11.9 • 11.8

the quality of input features, whereas deeper networks may require more carefully engineered inputs.

Table 5 shows a comparison of the present study results with other research studies in the literature. All models are compared using RMSE values (after converting it to W/m²). Inputs considered in each study are similar however, time horizons are different. It is noted that the error increases when the time span increases. Moreover, the LSTM is found to be better for very short time horizons while GRU achieved better results for longer time horizons. The trained models presented in this study give less error than the other models as more inputs are considered and the efficiency of the followed training strategy. Although this study used satellite data which might deviate from the real measured data at the site; it shows the efficiency of the proposed models for forecasting the daily solar irradiance. However, further investigation can be carried out by comparing the results to actual meteorological data to get the exact error of the models which are not available in the present case.

V. CONCLUSION

Deep Learning Techniques are investigated in this study for solar irradiance forecasting problem, and the results are validated using data from a hilly location in India. A comparative analysis and validation of three reliable deep learning techniques, MLP, LSTM and GRU are presented. The DL techniques are implemented to find the most competitive one to forecast daily GHI accurately for any location. The models are trained and tested using satellite solar irradiance data, and

the grid search technique is followed to find the optimum architectures. The main conclusions are as follows:

- Based on the literature review, the best three architectures with high accuracy are identified as MLP, LSTM, GRU networks.
- Grid search technique is used efficiently to optimize the models' architectures that meet the complexity of the problem.
- By optimizing the model architecture, the three networks are able to achieve similar forecasting accuracy of the daily global solar irradiance.
- MLP is found to be the simplest network with the least number of hyperparameters and the fastest training time.
- Different parameters such as direct normal irradiance or diffuse solar irradiance can also be predicted in the same manner.

The proposed networks can also be used for different time horizon forecasting to be applied for demand and supply balancing or for energy management purposes. Moreover, the results can be compared to the meteorological data to assess the proposed models and identify the real models' accuracy based on measured data. Further follow-up research can be undertaken for solar radiation forecasting for any location worldwide using NASA data. Finally, grid search technology may not be effective when a high number of parameters is taken, therefore, metaheuristic techniques can be used to optimize the DL techniques' architectures.

Moreover, as energy generation, storage, and consumption become more integrated, forecasting systems will evolve to manage these interconnections effectively. Given the uncertainty associated with climate change, future models may focus on adaptability and resilience, helping systems cope up with extreme weather events. The future trends in short-term solar irradiance forecasting using deep learning techniques are expected to focus on accuracy, real-time capabilities, and adaptability to changing environmental conditions. Additionally, there will be a growing emphasis on transparency and understanding the models' decision-making processes, especially in applications affecting energy grids and infrastructure.

ACKNOWLEDGMENT

The authors extend their appreciation to the Researchers Supporting Project at King Saud University, Riyadh, Saudi Arabia, for funding this research work through the project number RSP2023R278. They would also like to acknowledge the technical support from Intelligent Prognostic Private Ltd., Delhi, India, researcher's supporting project for this research work; and the technical support from Ingenium Research Group, Universidad Castilla-La Mancha, Ciudad Real, Spain.

REFERENCES

- [1] E. Kabir, P. Kumar, S. Kumar, A. A. Adelodun, and K.-H. Kim, "Solar energy: Potential and future prospects," *Renew. Sustain. Energy Rev.*, vol. 82, pp. 894–900, Feb. 2018, doi: [10.1016/j.rser.2017.09.094](https://doi.org/10.1016/j.rser.2017.09.094).
- [2] T. Blaschke, M. Biberacher, S. Gadocha, and I. Schardinger, "Energy landscapes': Meeting energy demands and human aspirations," *Biomass Bioenergy*, vol. 55, pp. 3–16, Aug. 2013, doi: [10.1016/j.biombioe.2012.11.022](https://doi.org/10.1016/j.biombioe.2012.11.022).
- [3] M. A. Al-Tameemi and V. V. Chukin, "Global water cycle and solar activity variations," *J. Atmos. Solar-Terr. Phys.*, vol. 142, pp. 55–59, May 2016, doi: [10.1016/j.jastp.2016.02.023](https://doi.org/10.1016/j.jastp.2016.02.023).
- [4] M. Hart, *Hubris: The Troubling Science, Economics, and Politics of Climate Change*. Philadelphia, PA, USA: Compleat Desktops Publishing, 2015.
- [5] S. Tadjour and S. S. Chandel, "A comprehensive review on sustainable energy management systems for optimal operation of future-generation of solar microgrids," *Sustain. Energy Technol. Assessments*, vol. 58, Aug. 2023, Art. no. 103377, doi: [10.1016/J.SETA.2023.103377](https://doi.org/10.1016/J.SETA.2023.103377).
- [6] S. S. Chandel, R. K. Aggarwal, and A. N. Pandey, "A new approach to estimate global solar radiation on horizontal surfaces from temperature data," *J. Solar Energy Soc. India*, vol. 12, no. 2, p. 109, 2002.
- [7] S. S. Chandel and R. K. Aggarwal, "Estimation of hourly solar radiation on horizontal and inclined surfaces in western Himalayas," *Smart Grid Renew. Energy*, vol. 2, no. 1, pp. 45–55, 2011, doi: [10.4236/sgre.2011.21006](https://doi.org/10.4236/sgre.2011.21006).
- [8] S. Tadjour, S. S. Chandel, H. Malik, M. A. Alotaibi, and T. S. Ustun, "A novel metaheuristic approach for solar photovoltaic parameter extraction using manufacturer data," *Photonics*, vol. 9, no. 11, p. 858, Nov. 2022, doi: [10.3390/photonics9110858](https://doi.org/10.3390/photonics9110858).
- [9] C. Sweeney, R. J. Bessa, J. Browell, and P. Pinson, "The future of forecasting for renewable energy," *WIREs Energy Environ.*, vol. 9, no. 2, pp. 1–10, Mar. 2020, doi: [10.1002/WENE.365](https://doi.org/10.1002/WENE.365).
- [10] B. Joshi, M. Kay, J. K. Copper, and A. B. Sproul, "Evaluation of solar irradiance forecasting skills of the Australian bureau of meteorology's ACCESS models," *Sol. Energy*, vol. 188, pp. 386–402, Aug. 2019, doi: [10.1016/J.SOLENER.2019.06.007](https://doi.org/10.1016/J.SOLENER.2019.06.007).
- [11] R. Tawn and J. Browell, "A review of very short-term wind and solar power forecasting," *Renew. Sustain. Energy Rev.*, vol. 153, Jan. 2022, Art. no. 111758, doi: [10.1016/J.RSER.2021.111758](https://doi.org/10.1016/J.RSER.2021.111758).
- [12] D. Chandola, H. Gupta, V. A. Tikkiwal, and M. K. Bohra, "Multi-step ahead forecasting of global solar radiation for arid zones using deep learning," *Proc. Comput. Sci.*, vol. 167, pp. 626–635, Jan. 2020, doi: [10.1016/j.procs.2020.03.329](https://doi.org/10.1016/j.procs.2020.03.329).
- [13] T. C. McCandless, S. E. Haupt, and G. S. Young, "A model tree approach to forecasting solar irradiance variability," *Sol. Energy*, vol. 120, pp. 514–524, Oct. 2015, doi: [10.1016/J.SOLENER.2015.07.020](https://doi.org/10.1016/J.SOLENER.2015.07.020).
- [14] S. Tadjour and S. Chandel, "Power generation forecasting of a solar photovoltaic power plant by a novel transfer learning technique with small solar radiation and power generation training data sets," *SSRN Electron. J.*, vol. 2022, pp. 1–27, Feb. 2022, doi: [10.2139/ssrn.4024225](https://doi.org/10.2139/ssrn.4024225).
- [15] A. K. Yadav and S. S. Chandel, "Solar radiation prediction using artificial neural network techniques: A review," *Renew. Sustain. Energy Rev.*, vol. 33, pp. 772–781, May 2014, doi: [10.1016/j.rser.2013.08.055](https://doi.org/10.1016/j.rser.2013.08.055).
- [16] A. K. Yadav, H. Malik, and S. S. Chandel, "ANN based prediction of daily global solar radiation for photovoltaics applications," in *Proc. Annu. IEEE India Conf. (INDICON)*, Dec. 2015, pp. 1–5.
- [17] A. K. Yadav, H. Malik, and S. S. Chandel, "Selection of most relevant input parameters using WEKA for artificial neural network based solar radiation prediction models," *Renew. Sustain. Energy Rev.*, vol. 31, pp. 509–519, Mar. 2014, doi: [10.1016/j.rser.2013.12.008](https://doi.org/10.1016/j.rser.2013.12.008).
- [18] A. K. Yadav, H. Malik, and S. S. Chandel, "Application of rapid miner in ANN based prediction of solar radiation for assessment of solar energy resource potential of 76 sites in northwestern India," *Renew. Sustain. Energy Rev.*, vol. 52, pp. 1093–1106, Dec. 2015, doi: [10.1016/j.rser.2015.07.156](https://doi.org/10.1016/j.rser.2015.07.156).
- [19] C. Voyant, G. Nottin, S. Kalogirou, M.-L. Nivet, C. Paoli, F. Motte, and A. Fouilloy, "Machine learning methods for solar radiation forecasting: A review," *Renew. Energy*, vol. 105, pp. 569–582, May 2017, doi: [10.1016/j.renene.2016.12.095](https://doi.org/10.1016/j.renene.2016.12.095).
- [20] M. Guermoui, F. Melgani, K. Gairaa, and M. L. Mekhalfi, "A comprehensive review of hybrid models for solar radiation forecasting," *J. Cleaner Prod.*, vol. 258, Jun. 2020, Art. no. 120357, doi: [10.1016/j.jclepro.2020.120357](https://doi.org/10.1016/j.jclepro.2020.120357).
- [21] D. S. Kumar, G. M. Yagli, M. Kashyap, and D. Srinivasan, "Solar irradiance resource and forecasting: A comprehensive review," *IET Renew. Power Gener.*, vol. 14, no. 10, pp. 1641–1656, Jul. 2020, doi: [10.1049/iet-rpg.2019.1227](https://doi.org/10.1049/iet-rpg.2019.1227).

- [22] O. Bamişile, A. Oluwasanmi, C. Ejayi, N. Yimen, S. Obiora, and Q. Huang, "Comparison of machine learning and deep learning algorithms for hourly global/diffuse solar radiation predictions," *Int. J. Energy Res.*, vol. 46, no. 8, pp. 1–22, Jun. 2021, doi: [10.1002/er.6529](https://doi.org/10.1002/er.6529).
- [23] R. A. Rajagukguk, R. A. A. Ramadhan, and H.-J. Lee, "A review on deep learning models for forecasting time series data of solar irradiance and photovoltaic power," *Energies*, vol. 13, no. 24, p. 6623, Dec. 2020, doi: [10.3390/en13246623](https://doi.org/10.3390/en13246623).
- [24] T. C. Carneiro, P. C. M. de Carvalho, H. Alves dos Santos, M. A. F. B. Lima, and A. P. D. S. Braga, "Review on photovoltaic power and solar resource forecasting: Current status and trends," *J. Sol. Energy Eng.*, vol. 144, no. 1, pp. 1–87, Feb. 2022.
- [25] H. T. C. Pedro and C. F. M. Coimbra, "Assessment of forecasting techniques for solar power production with no exogenous inputs," *Sol. Energy*, vol. 86, no. 7, pp. 2017–2028, Jul. 2012, doi: [10.1016/j.solener.2012.04.004](https://doi.org/10.1016/j.solener.2012.04.004).
- [26] D. Liu and K. Sun, "Random forest solar power forecast based on classification optimization," *Energy*, vol. 187, Nov. 2019, Art. no. 115940, doi: [10.1016/j.energy.2019.115940](https://doi.org/10.1016/j.energy.2019.115940).
- [27] M. Rana, I. Koprinska, and V. G. Agelidis, "2D-interval forecasts for solar power production," *Sol. Energy*, vol. 122, pp. 191–203, Dec. 2015, doi: [10.1016/j.solener.2015.08.018](https://doi.org/10.1016/j.solener.2015.08.018).
- [28] M. A. F. B. Lima, P. C. M. Carvalho, L. M. Fernández-Ramírez, and A. P. S. Braga, "Improving solar forecasting using deep learning and portfolio theory integration," *Energy*, vol. 195, Mar. 2020, Art. no. 117016, doi: [10.1016/j.energy.2020.117016](https://doi.org/10.1016/j.energy.2020.117016).
- [29] Y. Jung, J. Jung, B. Kim, and S. Han, "Long short-term memory recurrent neural network for modeling temporal patterns in long-term power forecasting for solar PV facilities: Case study of South Korea," *J. Cleaner Prod.*, vol. 250, Mar. 2020, Art. no. 119476, doi: [10.1016/j.jclepro.2019.119476](https://doi.org/10.1016/j.jclepro.2019.119476).
- [30] M. Gao, J. Li, F. Hong, and D. Long, "Day-ahead power forecasting in a large-scale photovoltaic plant based on weather classification using LSTM," *Energy*, vol. 187, Nov. 2019, Art. no. 115838, doi: [10.1016/j.energy.2019.07.168](https://doi.org/10.1016/j.energy.2019.07.168).
- [31] K. Wang, X. Qi, and H. Liu, "A comparison of day-ahead photovoltaic power forecasting models based on deep learning neural network," *Appl. Energy*, vol. 251, Oct. 2019, Art. no. 113315, doi: [10.1016/j.apenergy.2019.113315](https://doi.org/10.1016/j.apenergy.2019.113315).
- [32] M. A. Jallal, A. E. Yassini, S. Chabaa, A. Zeroual, and S. Ibnyach, "AI data driven approach-based endogenous inputs for global solar radiation forecasting," *Ingénierie Systèmes Inf.*, vol. 25, no. 1, pp. 27–34, Feb. 2020, doi: [10.18280/isi.250104](https://doi.org/10.18280/isi.250104).
- [33] O. Kisi, M. Alizamir, S. Trajkovic, J. Shiri, and S. Kim, "Solar radiation estimation in Mediterranean climate by weather variables using a novel Bayesian model averaging and machine learning methods," *Neural Process. Lett.*, vol. 52, no. 3, pp. 2297–2318, Dec. 2020, doi: [10.1007/s11063-020-10350-4](https://doi.org/10.1007/s11063-020-10350-4).
- [34] Ü. Ağbulut, A. E. Gürel, and Y. Biçen, "Prediction of daily global solar radiation using different machine learning algorithms: Evaluation and comparison," *Renew. Sustain. Energy Rev.*, vol. 135, Jan. 2021, Art. no. 110114, doi: [10.1016/j.rser.2020.110114](https://doi.org/10.1016/j.rser.2020.110114).
- [35] M. Alizamir, S. Kim, O. Kisi, and M. Zounemat-Kermani, "A comparative study of several machine learning based non-linear regression methods in estimating solar radiation: Case studies of the USA and Turkey regions," *Energy*, vol. 197, Apr. 2020, Art. no. 117239, doi: [10.1016/j.energy.2020.117239](https://doi.org/10.1016/j.energy.2020.117239).
- [36] Y. Yu, J. Cao, and J. Zhu, "An LSTM short-term solar irradiance forecasting under complicated weather conditions," *IEEE Access*, vol. 7, pp. 145651–145666, 2019, doi: [10.1109/ACCESS.2019.2946057](https://doi.org/10.1109/ACCESS.2019.2946057).
- [37] M. Aslam, J.-M. Lee, H.-S. Kim, S.-J. Lee, and S. Hong, "Deep learning models for long-term solar radiation forecasting considering microgrid installation: A comparative study," *Energies*, vol. 13, no. 1, p. 147, Dec. 2019, doi: [10.3390/en13010147](https://doi.org/10.3390/en13010147).
- [38] S. Monjoly, M. André, R. Calif, and T. Soubdhan, "Hourly forecasting of global solar radiation based on multiscale decomposition methods: A hybrid approach," *Energy*, vol. 119, pp. 288–298, Jan. 2017, doi: [10.1016/j.energy.2016.11.061](https://doi.org/10.1016/j.energy.2016.11.061).
- [39] S. E. Berrizbeitia, E. J. Gago, and T. Muneer, "Empirical models for the estimation of solar sky-diffuse radiation. A review and experimental analysis," *Energies*, vol. 13, no. 3, p. 701, Feb. 2020, doi: [10.3390/en13030701](https://doi.org/10.3390/en13030701).
- [40] S. Bamehr and S. Sabetghadam, "Estimation of global solar radiation data based on satellite-derived atmospheric parameters over the urban area of Mashhad, Iran," *Environ. Sci. Pollut. Res.*, vol. 28, no. 6, pp. 7167–7179, Feb. 2021, doi: [10.1007/s11356-020-11003-8](https://doi.org/10.1007/s11356-020-11003-8).
- [41] J. Marcello, F. Eugenio, and F. Marques, "Cloud motion estimation in SEVIRI image sequences," in *Proc. IEEE Int. Geosci. Remote Sens. Symp.*, Jul. 2009, pp. 642–645, doi: [10.1109/IGARSS.2009.5417842](https://doi.org/10.1109/IGARSS.2009.5417842).
- [42] J. L. Bosch and J. Kleissl, "Cloud motion vectors from a network of ground sensors in a solar power plant," *Sol. Energy*, vol. 95, pp. 13–20, Sep. 2013, doi: [10.1016/j.solener.2013.05.027](https://doi.org/10.1016/j.solener.2013.05.027).
- [43] M. Guermoui, K. Gairaa, J. Boland, and T. Arrif, "A novel hybrid model for solar radiation forecasting using support vector machine and bee colony optimization algorithm: Review and case study," *J. Sol. Energy Eng.*, vol. 143, no. 2, pp. 1–20, Apr. 2021, doi: [10.1115/1.4047852](https://doi.org/10.1115/1.4047852).
- [44] Y. Feng, W. Hao, H. Li, N. Cui, D. Gong, and L. Gao, "Machine learning models to quantify and map daily global solar radiation and photovoltaic power," *Renew. Sustain. Energy Rev.*, vol. 118, Feb. 2020, Art. no. 109393, doi: [10.1016/j.rser.2019.109393](https://doi.org/10.1016/j.rser.2019.109393).
- [45] Z. Dong, D. Yang, T. Reindl, and W. M. Walsh, "A novel hybrid approach based on self-organizing maps, support vector regression and particle swarm optimization to forecast solar irradiance," *Energy*, vol. 82, pp. 570–577, Mar. 2015, doi: [10.1016/j.energy.2015.01.066](https://doi.org/10.1016/j.energy.2015.01.066).
- [46] H. Lan, C. Zhang, Y.-Y. Hong, Y. He, and S. Wen, "Day-ahead spatiotemporal solar irradiation forecasting using frequency-based hybrid principal component analysis and neural network," *Appl. Energy*, vol. 247, pp. 389–402, Aug. 2019, doi: [10.1016/j.apenergy.2019.04.056](https://doi.org/10.1016/j.apenergy.2019.04.056).
- [47] F. Baser and H. Demirhan, "A fuzzy regression with support vector machine approach to the estimation of horizontal global solar radiation," *Energy*, vol. 123, pp. 229–240, Mar. 2017, doi: [10.1016/j.energy.2017.02.008](https://doi.org/10.1016/j.energy.2017.02.008).
- [48] S. Bhardwaj, V. Sharma, S. Srivastava, O. S. Sastry, B. Bandyopadhyay, S. S. Chandel, and J. R. P. Gupta, "Estimation of solar radiation using a combination of hidden Markov model and generalized fuzzy model," *Sol. Energy*, vol. 93, pp. 43–54, Jul. 2013, doi: [10.1016/j.solener.2013.03.020](https://doi.org/10.1016/j.solener.2013.03.020).
- [49] V. Gunasekaran, K. K. Kovi, S. Arja, and R. Chimata, "Solar irradiation forecasting using genetic algorithms," 2021, *arXiv:2106.13956*.
- [50] W. S. McCulloch and P. Walter, "A logical calculus of the ideas immanent in nervous activity," in *Proc. Int. Conf. Intell. Auton. Syst.*, in Advances in Intelligent Systems and Computing, vol. 5, 1943, pp. 786–798, doi: [10.1007/978-3-030-01370-7_61](https://doi.org/10.1007/978-3-030-01370-7_61).
- [51] S. Tajjour, S. Garg, S. S. Chandel, and D. Sharma, "A novel hybrid artificial neural network technique for the early skin cancer diagnosis using color space conversions of original images," *Int. J. Imag. Syst. Technol.*, vol. 33, no. 1, pp. 1–11, Jul. 2022, doi: [10.1002/ima.22784](https://doi.org/10.1002/ima.22784).
- [52] A. Aksoy, Y. E. Ertürk, S. Erdoğan, E. Eydurhan, and M. M. Tariq, "Estimation of honey production in beekeeping enterprises from eastern part of Turkey through some data mining algorithms," *Pakistan J. Zool.*, vol. 50, no. 6, pp. 2199–2207, 2018, doi: [10.17582/journal.pjz/2018.50.6.2199.2207](https://doi.org/10.17582/journal.pjz/2018.50.6.2199.2207).
- [53] K. Cho, B. van Merriënboer, C. Gulcehre, D. Bahdanau, F. Bougares, H. Schwenk, and Y. Bengio, "Learning phrase representations using RNN encoder-decoder for statistical machine translation," in *Proc. Conf. Empirical Methods Natural Lang. Process. (EMNLP)*, 2014, pp. 1724–1734, doi: [10.3115/v1/d14-1179](https://doi.org/10.3115/v1/d14-1179).
- [54] X. Qing and Y. Niu, "Hourly day-ahead solar irradiance prediction using weather forecasts by LSTM," *Energy*, vol. 148, pp. 461–468, Apr. 2018, doi: [10.1016/j.energy.2018.01.177](https://doi.org/10.1016/j.energy.2018.01.177).
- [55] J. Wojtkiewicz, M. Hosseini, R. Gottumukkala, and T. L. Chambers, "Hour-ahead solar irradiance forecasting using multivariate gated recurrent units," *Energies*, vol. 12, no. 21, pp. 1–13, 2019, doi: [10.3390/en12214055](https://doi.org/10.3390/en12214055).
- [56] H. He, N. Lu, Y. Jie, B. Chen, and R. Jiao, "Probabilistic solar irradiance forecasting via a deep learning-based hybrid approach," *IEEE Trans. Electr. Electron. Eng.*, vol. 15, no. 11, pp. 1604–1612, Nov. 2020, doi: [10.1002/tee.23231](https://doi.org/10.1002/tee.23231).
- [57] M. Husein and I.-Y. Chung, "Day-ahead solar irradiance forecasting for microgrids using a long short-term memory recurrent neural network: A deep learning approach," *Energies*, vol. 12, no. 10, p. 1856, May 2019, doi: [10.3390/en12101856](https://doi.org/10.3390/en12101856).
- [58] K. Yan, H. Shen, L. Wang, H. Zhou, M. Xu, and Y. Mo, "Short-term solar irradiance forecasting based on a hybrid deep learning methodology," *Information*, vol. 11, no. 1, pp. 1–13, 2020, doi: [10.3390/info11010032](https://doi.org/10.3390/info11010032).

•••